Malaysian Journal of Chemistry, 2026, Vol. 28(4), 64-74

Hydrogen Generation by Catalytic Hydrolysis of $NaBH_4$ with *h*-BN-Supported CoB

Nor Izzati Nordin[1], Ee Loong Koh[1], Usman Lado Ali[1], Yunfeng Lei[1], Huilin Liu[1], Wen Da Oh[2], Hooi Ling Lee[2] and Yong Shen Chua[1]*

[1]Hydrogen Energy Storage Research Group, School of Chemical Sciences, Universiti Sains Malaysia, 11800 Minden, Penang, Malaysia

[2]School of Chemical Sciences, Universiti Sains Malaysia, 11800 Minden, Penang, Malaysia

*Corresponding author (e-mail: yschua@usm.my)

Sodium borohydride ($NaBH_4$) is emerging as a highly promising hydrogen storage material due to its exceptional gravimetric hydrogen storage capacity (10.7 wt%). Its ability to rapidly release hydrogen through hydrolysis under ambient conditions makes it an ideal candidate for on-demand power generation in fuel cells. However, without a catalyst, the hydrolysis kinetics of $NaBH_4$ remain slow. Traditionally, Co-B alloy has been used as an effective catalyst, though it tends to agglomerate, reducing both activity and durability. In this study, amorphous hexagonal boron nitride (*h*-BN) was successfully synthesized and employed as a support material to improve the stability of Co particles, forming the Co/BN catalyst. A systematic investigation of transition metal-based catalysts (Co/BN, Ni/BN, Cu/BN, and Sn/BN) for $NaBH_4$ hydrolysis revealed 10 wt% Co/BN as the most active catalyst, achieving a hydrogen yield of 3.6 mol H_2/mol $NaBH_4$ at 30 °C with an activation energy of 29.23 kJ mol^{-1}. These findings provide valuable insights into catalytic mechanisms and contribute to the development of an efficient, cost-effective hydrogen production method using Co-based catalysts in heterogeneous reactions.

Keywords: Hydrogen storage, hydrolysis, borohydrides, catalysis, boron nitride

Received: January 2026; Accepted: March 2026

Nowadays, the use of fossil fuels and oil as primary energy sources has reached its peak, raising serious concerns such as the depletion of global reserves and the environmental impacts of their combustion. Hydrogen has emerged as a promising alternative due to its high energy density and zero-emission potential when used in fuel cells. Among various chemical hydrogen storage methods, sodium borohydride ($NaBH_4$) is considered one of the most promising due to its high gravimetric hydrogen storage capacity (10.7 wt%) and ease of handling [1]. Additionally, the by-product, sodium metaborate, is water-soluble and environmentally friendly [2]. $NaBH_4$ hydrolysis, which produces hydrogen gas upon reaction with water, offers a practical approach for on-demand hydrogen generation. It is well documented that in the hydrolysis of $NaBH_4$, an increase in system temperature is unavoidable. When water is added to $NaBH_4$ pellets, the evolving heat from the reaction cannot be effectively dissipated, resulting in a significant increase in the reactor temperature [3]. Leveraging on its high latent heat of vaporization, water appears to be the ideal heat sink to prevent overaccumulation of heat in the solid state $NaBH_4$ reservoir.

A large body of research has focused on the use of $NaBH_4$ aqueous solutions, where $NaBH_4$ is pre-dissolved in an alkaline solution which is introduced to the catalyst for hydrogen production on demand. While the use of aqueous alkaline $NaBH_4$ solutions has been effective, it presents several practical challenges, as hydrolysis cannot be completely suppressed even under alkaline conditions. For instance, up to 66 % of $NaBH_4$ has been reported to hydrolyze when an aqueous solution containing 15 wt% $NaBH_4$ and 5 wt% NaOH was stored for one year at 23–25 °C [4]. Long-term storage of $NaBH_4$ in aqueous alkaline solution is highly undesirable as it may pose safety risks due to uncontrolled hydrogen release. In addition, high-pH conditions have been reported to rapidly deactivate catalysts during the hydrolysis of alkali-stabilized $NaBH_4$ solutions, as exemplified by Co–B, markedly diminishing their catalytic performance [5]. Furthermore, the large amounts of water and NaOH used substantially reduce the practical gravimetric hydrogen capacity relative to the theoretical value. Although slow degradation may still occur in the presence of moisture, solid-state $NaBH_4$ offers enhanced storage stability compared with its aqueous counterpart, making its hydrolysis a more practical approach [6]. This approach also eliminates the need for high-pressure storage tanks, as hydrogen can be generated at ambient pressure through the controlled hydrolysis of $NaBH_4$ pellets without the use of NaOH as a stabilizer. Such a strategy provides significant advantages for mobile or decentralized hydrogen generation systems, where compact and reliable storage solutions are essential.

Hydrolysis of $NaBH_4$ under ambient conditions is highly favourable for fuel cell applications, but one significant challenge is its slow reaction kinetics without a suitable catalyst [7]. Developing an efficient catalyst for $NaBH_4$ hydrolysis is essential for implementing this system in clean energy applications. Noble metal catalysts such as platinum (Pt) and ruthenium (Ru) have been shown to be effective, but their high cost and limited availability restrict their use in large-scale hydrogen production [2,8]. Despite these challenges, noble metal catalysts remain a benchmark for catalytic performance in hydrogen generation. In order to address this, researchers have turned to non-noble metal catalysts, including Co−B [9], Co_3O_4 [10], Co−P−B [11], Co−Fe−B [12], Ni−B [13], and Ni nanoparticles [14]. Co-based catalysts have attracted considerable attention because they can rapidly form Co–B during $NaBH_4$ hydrolysis, with $NaBH_4$ also serving as the reducing agent for the Co salt precursor [5]. However, Co–B is prone to agglomeration, which diminishes both catalytic activity and durability [5]. In heterogeneous catalysis, the choice of support is crucial, as it governs metal dispersion and the strength of metal–support interactions (SMSI). Two-dimensional hexagonal boron nitride (*h*-BN), a graphite-like layered material, has emerged as an attractive catalyst support due to its thermal robustness, chemical stability, high surface area, and tuneable surface properties [15]. These characteristics facilitate effective stabilization of metal nanoparticles and allow fine-tuning of their catalytic behaviour. Beyond its applications in adsorption and environmental remediation, [16,17] *h*-BN has also been widely explored as a catalyst support for hydrogen generation reactions. In particular, *h*-BN-supported catalysts such as Ru/*h*-BN [18], Ni@*h*-BN [15], and CuNi/*h*-BN [19] have shown enhanced catalytic performance in the hydrolysis of ammonia borane (NH_3BH_3), exhibiting lower hydrogen release temperatures and shorter induction periods. These findings highlight the potential of *h*-BN as an effective support for catalytic hydrogen generation. However, the application of *h*-BN-supported catalysts for $NaBH_4$ hydrolysis remains largely unexplored.

Therefore, in this study, the hydrolysis of solid-state $NaBH_4$ was investigated by introducing $NaBH_4$ pellets into an alkali-free aqueous solution containing various *h*-BN-supported transition metal catalysts (Co, Ni, Cu and Sn).

EXPERIMENTAL

Chemicals and Materials

All the chemicals and reagents used were of analytical grade and used as received. Boric acid (H_3BO_3, 99.5 %), urea (NH_2CONH_2, 99.5 %), copper (II) chloride ($CuCl_2$, 99 %) and sodium hydroxide (NaOH) were procured from R&M Chemicals. Nickel (II) chloride ($NiCl_2$, 98 %), tin (II) chloride ($SnCl_2$, 97 %) and sodium borohydride ($NaBH_4$, 96 %) were obtained from Sigma-Aldrich (United Kingdom). Anhydrous cobalt (II) chloride ($CoCl_2$, 97 %) was supplied by ACROS Organics.

Synthesis of Boron Nitride as Catalyst Support

Boron nitride was synthesized following the procedure reported by Wu and co-workers, which involved mixing boric acid and urea in a molar ratio of 1:30 [20]. Initially, 0.01 mol of H_3BO_3 and 0.30 mol of urea were dissolved in 40 mL of a solvent composed of methanol and water in a 1:1 volume ratio. The resulting homogeneous solution was heated in a water bath to 45 °C to promote recrystallization, yielding a white crystalline powder. This powder was then calcined at 900 °C with a heating rate of 5 °C/min under a nitrogen atmosphere. After 2 h of calcination, the tube furnace was allowed to cool naturally to room temperature, producing the hexagonal boron nitride product hereafter denoted as BN.

Preparation of Catalysts Supported on Boron Nitride

The as-prepared boron nitride was further doped with four different metals, yielding 5 wt% M/BN (M= Co, Ni, Sn, and Cu) using the precursors $CoCl_2$, $NiCl_2$, $SnCl_2$ and $CuCl_2$. Initially, 0.5 g of BN was dispersed in 100 mL of ultrapure water by sonicating for 1 h. The appropriate amount of metal salt e.g., $CoCl_2$ was then added to the solution and stirred for 6 h to ensure uniform dispersion of the metal precursor on the BN surface. After centrifugation and drying at 120 °C, the product was calcined at 650 °C under a nitrogen atmosphere for 2 h. The catalyst was further reduced using a $NaBH_4$ solution (10 mL of 0.2 M) and stirred for 1 hour. The resulting mixture was centrifuged and washed several times with ultrapure water and ethanol before being dried at 120 °C to yield the Co/BN catalyst. The same procedure was applied with different metals and different loadings of Co/BN.

Characterization Techniques

Prior to characterization, a preliminary catalytic screening for the hydrolysis of $NaBH_4$ was performed. The most active catalyst was then selected for detailed characterization. The chemical bonds and composition of the catalyst were analysed by Fourier Transform Infrared Spectroscopy (FTIR) using the Shimadzu IRSpirit A224160. The phase composition was determined on a Bruker D8 Advance X-ray powder diffractometer (XRD) with Cu-Kα, 40 kV and 40 mA. The morphology and EDX elemental distribution of the BN and catalyst were observed using an ultra-high resolution electron microscope (UHRSEM, Hitachi Regulus 8220) equipped with an electron dispersive spectroscopy detector (Oxford I6 instruments X-Max 80). X-ray photoelectron spectroscopy (XPS) was acquired using an AXIS Ultra DLD system (Kratos, UK) with an Al Kα X-ray source (1486.6 eV) at 10 mA and 14 kV. The analysis covered a 300 µm x 700

μm area under an ultra-high vacuum of 4.8E x 10^{-9} torr. The spectra were calibrated using the C1s binding energy (284.6 eV).

Hydrogen Generation Test

The catalytic performance of the as-synthesized catalyst was evaluated for hydrolysis of $NaBH_4$. The hydrolysis reaction was initially performed at 30 °C by reacting 0.2 g of $NaBH_4$ pellets with 20 mg of catalyst in 20 mL of distilled water. $NaBH_4$ was weighed in a glove box to prevent self-hydrolysis. The hydrolysis reaction was conducted in a stainless-steel reactor at a stirring speed of 100 rpm. The pressure increase during the hydrolysis reaction was monitored using a custom-made pressure release system equipped with a pressure data logger. The reaction was optimized for various parameters, including different metals supported on BN, varying metal loadings and the addition of NaOH. The kinetic evaluation was carried out by performing the hydrolysis reaction with varying initial $NaBH_4$ dosages and reaction temperatures to determine the reaction order and activation energy, respectively. The hydrolysis activation energy was investigated using the Co–B catalyst at different temperatures. The calculations and data analysis were performed as follows [6]:

The recorded pressure profile was used to calculate the number of moles of H_2 released using the ideal gas law (equation 1).

$$PV = nH_2 \times RT \quad (1)$$

The theoretical amount of H_2 generated was calculated based on the stoichiometry of the hydrolysis reaction, as given in equation 2.

$$nH_2\ (\text{mol}) = 4 \times \frac{NaBH_4\ \text{amount (g)}}{MWt\ NaBH_4(\frac{g}{mol})} \quad (2)$$

H_2 yield (%) is defined as the percentage of theoretical hydrogen generated from the hydrolysis reaction (equation 3).

$$H_2\ \text{yield (\%)} = \frac{\text{Total of } nH_2 \text{ generated}}{\text{Theoretical } nH_2 \text{ generated}} \quad (3)$$

The initial H_2 generation rate was determined from the H_2 evolution curve (equation 4).

$$\text{Initial } H_2 \text{ generation rate (mol } H_2\ min^{-1}) = \text{slope} = \frac{\Delta(nH_2/nNaBH_4)}{\Delta t} \quad (4)$$

RESULTS AND DISCUSSION

Catalytic Screening and Characterization

The hydrogen generation reaction from the hydrolysis of $NaBH_4$ is given in equation (5). The amount of hydrogen released can be easily monitored using a pressure release system. Theoretically, this exothermic process releases 4 mol equiv. H_2 per mol $NaBH_4$ along with sodium metaborate as a by-product. The catalytic performance of the as-prepared boron nitride (BN) was initially evaluated without the addition of a metal catalyst. As illustrated in Figure 1(a), BN accelerated the reaction rate compared to the non-catalyzed system, which showed significantly slower hydrogen release, emphasizing the need for a catalyst to speed up the process.

$$NaBH_4 + 2H_2O \rightarrow NaBO_2 \cdot H_2O + 4H_2 + \text{Heat} \quad (5)$$

The catalytic performance was further evaluated using different metal-supported boron nitride catalysts (Co, Ni, Cu, Sn) for the hydrolysis of sodium borohydride ($NaBH_4$). Among the catalysts studied, 5 wt% Co/BN exhibited the highest efficiency for $NaBH_4$ hydrolysis, releasing 3.6 mol H_2/mol $NaBH_4$ within 55 min (Figure 1(a)). In comparison, Ni/BN, Cu/BN, and Sn/BN released 3.4, 3.5, and 2.8 mol H_2/mol $NaBH_4$, respectively. The corresponding initial hydrogen generation rates followed the order Co/BN (0.266 mol H_2 min^{-1}) > Cu/BN (0.181 mol H_2 min^{-1}) > Ni/BN (0.150 mol H_2 min^{-1}) > Sn/BN (0.065 mol H_2 min^{-1}), highlighting the superior activity of Co/BN under the tested conditions. The exceptional performance of Co/BN was attributed to cobalt's ability to adsorb and activate borohydride anions, as well as its synergistic interaction with BN, which prevented nanoparticle aggregation and enhanced catalyst stability. Interestingly, the presence of cobalt nanoparticles significantly enhanced hydrolysis performance by providing additional active sites on the catalyst surface. BN served as a robust support, further improving efficiency and durability. This study demonstrated that while BN possessed inherent catalytic properties, its performance was significantly enhanced by Co doping, making Co/BN the most efficient catalyst in this context.

Preliminary catalytic screening in the hydrolysis of $NaBH_4$ showed that Co/BN exhibited significantly higher activity than the other prepared catalysts. Therefore, detailed characterization was carried out primarily on Co/BN as the most active catalyst. The FTIR analysis provided evidence of successful synthesis of Co/BN using urea and boric acid (Figure 1(b)). The most prominent N–H stretching band, carbonyl stretching at 3200-3600 cm^{-1} and 1668 cm^{-1}, respectively, which were initially observed in the nitrogen precursor, was absent in the synthesised product. The spectrum of boron nitride (BN) showed significant peaks at 1406 cm^{-1} corresponding to B–N stretching vibrations, and additional peaks between 703 cm^{-1} attributed to B–N bending vibrations, confirming the formation of BN and consistent with those reported by Singh and co-workers [16]. The broad absorption peak around 3200 cm^{-1} could be due to the O–H bond of water molecules adsorbed on the surface of boron nitride, which was also accompanied by a BN–O peak at 1192 cm^{-1} [16]. In addition, the Co/BN spectrum retained these BN features, indicating successful doping of cobalt on BN. Red shifts in the BN-associated peaks suggest interactions

between cobalt and BN, which affect their bond energy [21]. A reduced O–H peak in Co/BN indicates partial dehydroxylation during the process. Overall, the spectra confirmed the conversion of precursors into the desired Co/BN catalyst.

Figure 1(c) presents the XRD patterns for the synthesized catalyst, BN and Co/BN which showed no similarities to the patterns of the starting reagents such as boric acid and urea. The XRD pattern for as-synthesized BN closely matched the XRD pattern (ICDD 01-07-32095) reported by Singh and co-workers, displaying its most intense peaks around 27.8°, corresponding to the (002) planes of *h*-BN, along with additional peaks for the (001), (100), (004) and (103) planes [16]. Upon metal addition, a broad peak appeared between 10° and 40°, suggesting the presence of amorphous or poorly crystalline Co/BN, while the peaks at approximately 35.6° and 45.4° are attributed to the amorphous form of Co–B [1,22]. The shifts and reduced intensity of BN peaks in the Co/BN spectrum suggest interactions between cobalt and BN. Additionally, the strong diffraction peak at about 26.1° could be assigned to the graphite structure or active carbon which indicates that both Co–B and carbon were present in the catalyst [1,22]. The remaining peaks could be due to the traces of different crystal forms of cobalt oxide in the sample, such as CoO and Co_3O_4 [1,23]. Overall, the sample contained a mixture of mostly amorphous BN with some crystalline phases, indicating the BN synthesized was primarily amorphous graphite-like *h*-BN.

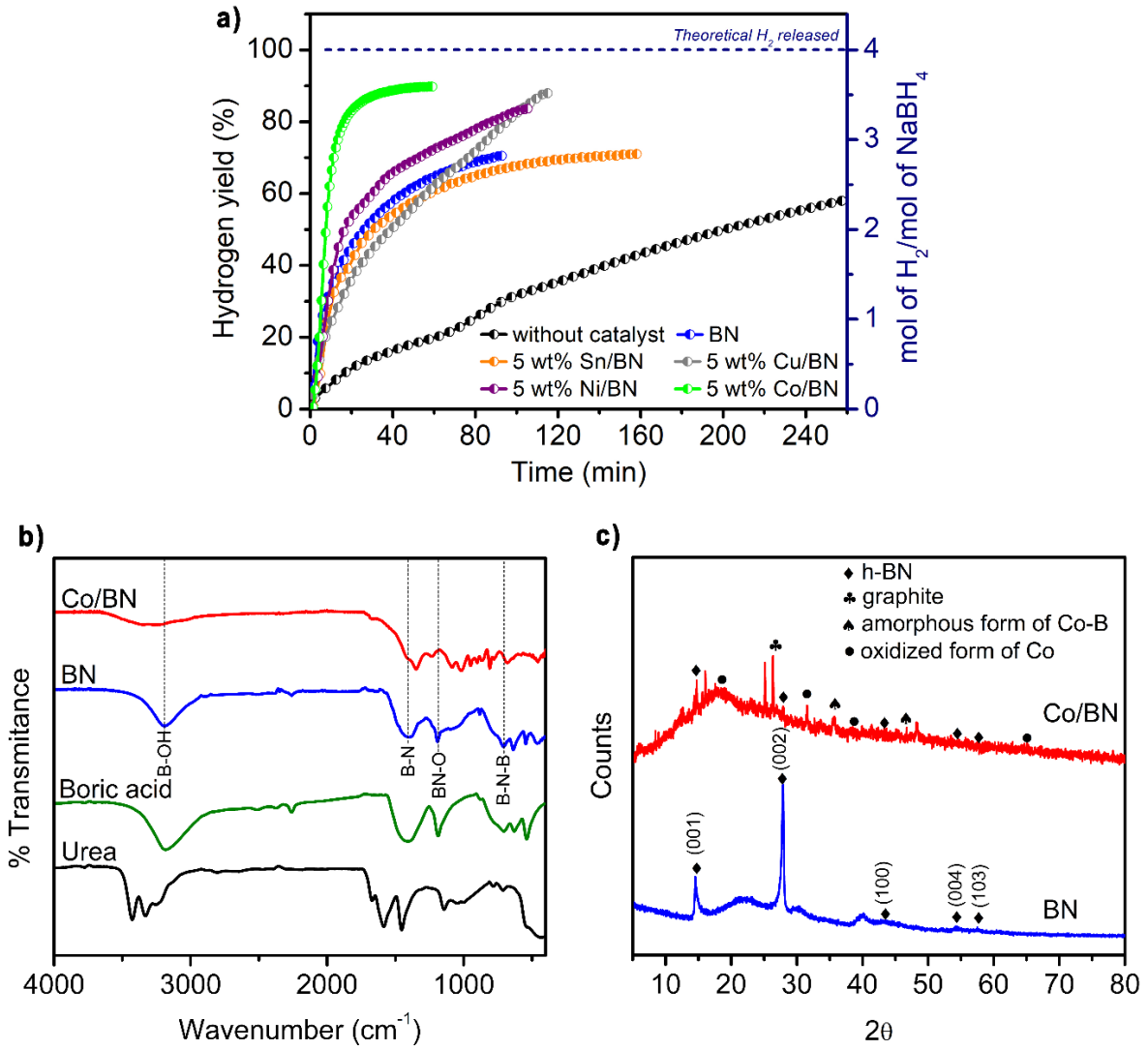

Figure 1. (a) Hydrolysis of $NaBH_4$ using different 5 wt% catalysts supported on boron nitride (0.2 g of $NaBH_4$ with 20 mg catalyst at 30 °C); (b) FTIR spectrum of as-synthesized BN, Co/BN compared to pristine boric acid and urea; (c) XRD pattern of as-synthesized BN and Co/BN.

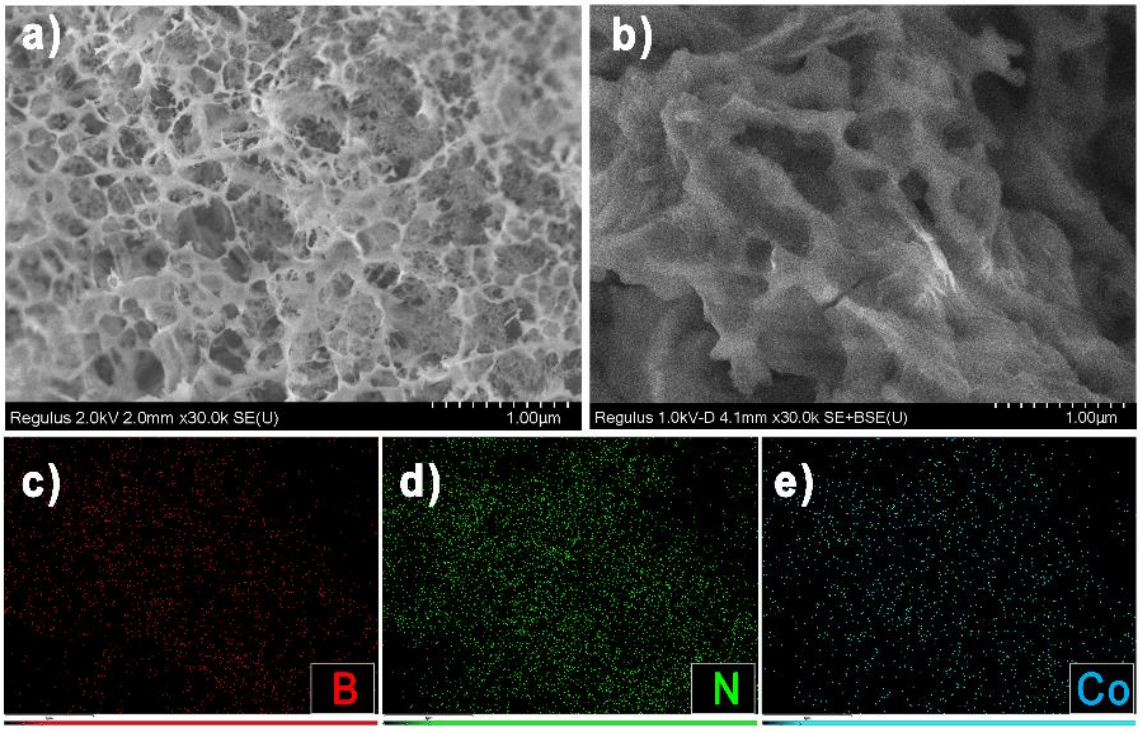

Figure 2. UHRSEM images of (a) BN and (b) Co/BN; (c-e) EDX element mapping of as-synthesized Co/BN.

The microstructure of the synthesized 1:30 boron nitride was confirmed by UHRSEM as shown in Figure 2(a). The SEM images of pure boron nitride show an interconnected network with a porous structure. The thin surface appeared relatively uniform with some occasional defects or imperfections observed. These were stacked in a staggered arrangement, forming numerous small voids with diameters ranging from ~0.1 to 0.5 µm in BN synthesized at 900 °C [24]. These voids are likely a result of raw material volatilization or the evolution of a gas such as NH_3 during the reaction, which typically originates from the nitrogen precursor at high temperatures [17,24]. Figure 2(b) shows the SEM image of cobalt deposited on boron nitride. The image reveals a notable change in the surface structure, which appeared denser, likely due to subsequent cobalt doping [25]. The EDX elemental distribution maps of Co/BN typically demonstrate that the cobalt particles appeared to be well-dispersed across the surface of the boron nitride, suggesting good interaction between cobalt and the BN substrate (Figure 2(c)-(e)). The mapping also indicates that the elemental B, N and Co particles were relatively small and uniformly distributed, which suggests the successful doping of Co on the BN surface using the wet impregnation method.

The chemical environment and major active sites in the as-synthesized Co–B catalyst were further investigated by XPS to evaluate their contribution to the radical generation and electron transfer during $NaBH_4$ hydrolysis. The full survey scan in Figure 3(a) revealed that Co, O, N, C, and B were the primary surface elements in the catalyst. The high-resolution, deconvoluted B 1s XPS spectrum showed multiple components corresponding to different boron environments, with peaks at 188.1, 191.1, 192.7, and 193.4 eV, assigned to boron in Co–B, B–C, BN and oxidized boron species, respectively (Figure 3(b)) [26–28]. Figure 3(c) shows the high-resolution N 1s spectrum, which can be deconvoluted into four types of nitrogen species corresponding to N–B bonding in *h*-BN motifs (398.5 eV), pyridinic–N (399.8 eV), pyrrolic–N (401.1 eV), and graphitic–N (402.3 eV) [27]. The presence of graphitic–N is consistent with the XRD results, which indicated that the as-prepared Co/BN catalyst also contained highly crystalline graphitic carbon. After curve deconvolution, the Co 2p spectrum (Figure 3d) was fitted with several peaks at 778.2, 781.6, 782.9, 785.9, 797.5, 799.1, and 803.4 eV. Notably, the small peak at 778.2 eV in the Co $2p_{3/2}$ region was assigned to the metallic Co–B species [29,30]. The remaining peaks at 781.6 eV and 782.9 eV, together with their broad satellite features at 785.9 and 803.4 eV, indicate the presence of oxidized cobalt species [28,30,31]. The spin-orbit splitting of 15.8 eV between the Co $2p_{3/2}$ and Co $2p_{1/2}$ components further confirmed that an oxidized cobalt species, likely Co^{3+}, dominated the surface. This is attributed to surface oxidation during catalyst preparation and exposure to air prior to XPS measurement, as well as the limited probing depth of XPS [21]. In the O 1s region (Figure 3(e)), three prominent peaks were observed at 531.9, 532.7, and 533.7 eV, attributed to lattice oxygen, substituted hydroxyl groups, and surface-adsorbed oxygen species, respectively [29].

Effect of Co Loading on BN Toward $NaBH_4$ Hydrolysis

The catalytic behaviour of the Co/BN catalyst on the hydrolysis of $NaBH_4$ was further investigated through comparative experiments and a kinetics study. To demonstrate the critical role of catalyst amount in the reaction, the effect of varying Co loadings on the BN catalyst for $NaBH_4$ hydrolysis was systematically investigated. Figure 4(a) shows that hydrogen generation improved significantly as the catalyst concentration increased from 1 wt% to 15 wt%. The 1 wt% Co/BN catalyst produced 3.1 mol H_2/mol $NaBH_4$, while the 5 wt% and 10 wt% Co/BN catalysts achieved yields of 3.5 and 3.6 mol H_2/mol $NaBH_4$, respectively. The optimal concentration was observed at 10 wt% Co/BN, which delivered the highest hydrogen yield (3.6 mol H_2/mol $NaBH_4$). Further increasing the concentration to 15 wt% resulted in minimal improvement, indicating saturation of active sites. The initial hydrogen generation rate was highest for the 10 wt% catalyst (0.4470 mol H_2 min^{-1}), whereas lower metal loadings, such as 1 wt%, provided fewer active sites and resulted in a slower hydrogen production rate of 0.3245 mol H_2 min^{-1}. Thus, 10 wt% Co/BN offered the optimal balance between catalyst loading and reaction efficiency, making it the most effective concentration for maximizing hydrogen production without the need for excess catalyst.

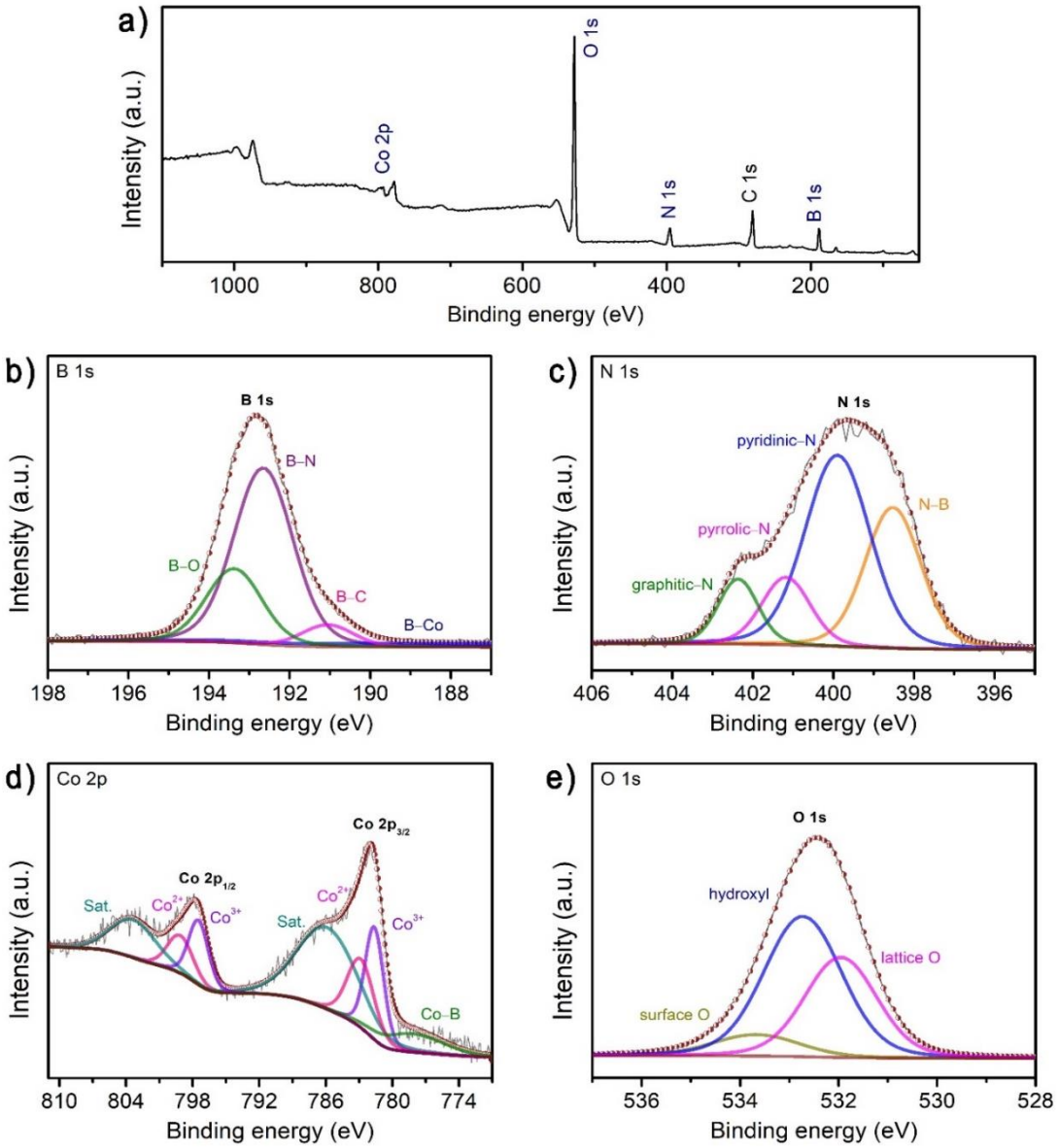

Figure 3. (a) XPS survey spectrum of as-synthesized Co/BN catalyst and the corresponding high-resolution XPS spectra of (b) B 1s, (c) N 1s, (d) Co 2p and (e) O 1s.

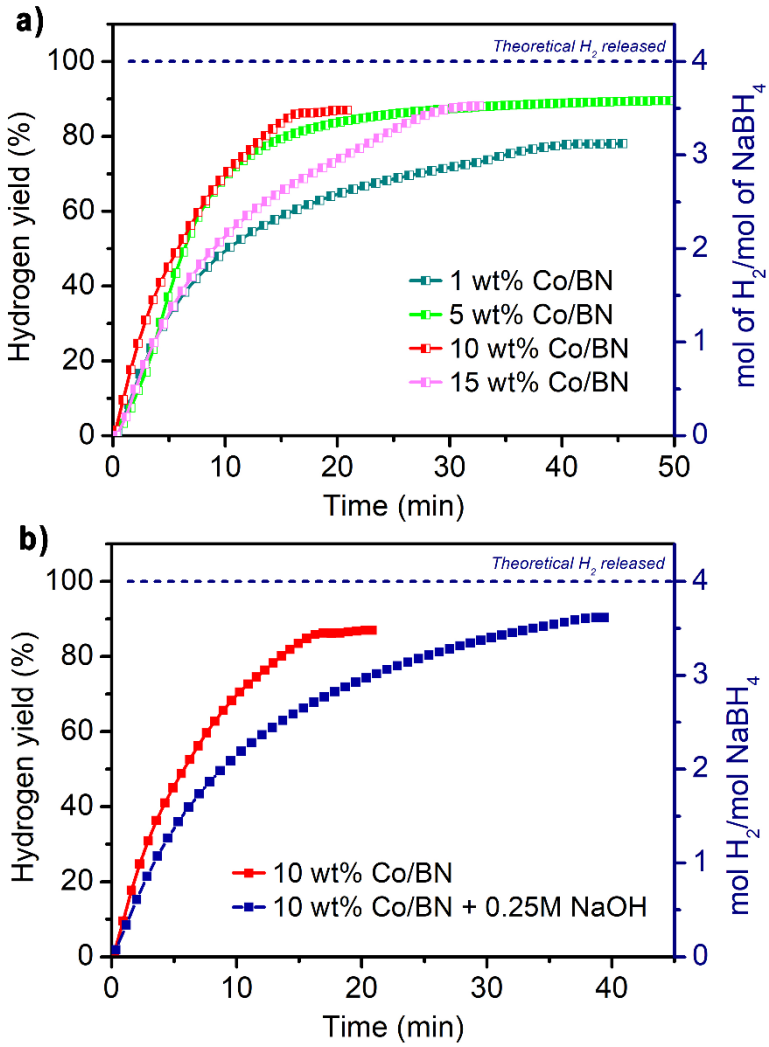

Figure 4. (a) Hydrolysis of $NaBH_4$ using four different amounts of Co on a BN metal catalyst, ranging from 1 to 15 wt% (0.2 g of $NaBH_4$ with 20 mg catalyst at 30 °C); (b) hydrolysis of $NaBH_4$ with 0.25 M NaOH (0.2 g of $NaBH_4$ with 20 mg 10 wt% Co/BN at 30 °C).

Effect of NaOH Concentration on $NaBH_4$ Hydrolysis

The effect of sodium hydroxide (NaOH) concentration on the catalytic activity of the Co/BN system was investigated, as shown in Figure 4(b). The reaction without NaOH exhibited a rapid hydrogen generation rate of 0.4470 mol H_2 min^{-1}, releasing 3.6 mol of H_2/mol $NaBH_4$ within 21 min. This suggests that in the absence of NaOH, $NaBH_4$ hydrolyzed quickly, leading to faster hydrogen release. In contrast, the addition of 0.25 M NaOH resulted in a slower initial rate of 0.3198 mol H_2 min^{-1}, but a more controlled and steady hydrogen production, culminating at approximately 3.0 mol equiv. H_2 over the same duration. While positive effects of NaOH addition on the hydrogen generation rate have been previously reported for Co and Ni-based catalysts, a negative effect has also been observed in Ru-catalyzed systems [8,32]. Although 0.25 M NaOH was reported to be effective for the Co–P–B catalyst, it was not effective for the present system [11]. Thus, the influence of NaOH concentration depends not only on the catalyst system but also on the catalyst support used. A high hydrogen generation rate can be achieved with an appropriate concentration of NaOH, which improves the dispersion of the supported catalysts. However, increasing the concentration of OH^- to strongly basic level is not recommended, as it raises the alkalinity and viscosity of the solution, thereby inhibiting the hydrolysis of $NaBH_4$ [33]. This phenomenon likely occurred in our study, as the pH of 0.25 M NaOH in 20 mL of water was approximately 13.4, which is strongly basic and not optimal for $NaBH_4$ hydrolysis. Previous studies by Sun and co-workers reported an optimal pH range of 7 to 10 and a temperature range of 15 to 35 °C for hydrolysis of $NaBH_4$ [3]. Additionally, when the NaOH concentration is too high, the active sites of the catalyst may be blocked by the precipitation of $NaBO_2$.

Kinetics Study

Based on recent research, the hydrolysis of $NaBH_4$ in aqueous alkaline solution involves $NaBH_4$, water, a catalyst and NaOH [34]. The rate of reaction can be expressed as a power law (Equation 6):

$$r = \frac{d[H_2]}{dt} = k[NaBH_4]^n \cdot [H_2O]^n \cdot [NaOH]^n \cdot [Catalyst]^n \quad (6)$$

In an excess of water (for example, a mole ratio of $H_2O/NaBH_4 \gg 50$), the term $[H_2O]^n$ could be seen as a constant. Since NaOH was not used in the hydrolysis of solid state $NaBH_4$, the term $[NaOH]^n$ can be removed from the rate equation. The effect of an increase in the catalyst amount on the reaction rate will not be discussed in detail in this article, as it is generally expected that an increase means more active sites and thus an improvement in kinetics [35]. The rate order with respect to the catalyst should be positive. Therefore, the rate equation becomes (Equation 7):

$$r = \frac{d[H_2]}{dt} = k\,[NaBH_4]^n \quad (7)$$

To accurately determine the reaction kinetics, the effect of varying the initial $NaBH_4$ dosage (0.1 – 0.3 g $NaBH_4$) on the reaction rate was investigated. As shown in Figure 5(a), the hydrogen generation rate was independent of the initial $NaBH_4$ dosage, indicating zero-order kinetics with respect to $NaBH_4$. Therefore, Equation 7 can be simplified to the following (Equation 8):

$$r = \frac{d[H_2]}{dt} = k \quad (8)$$

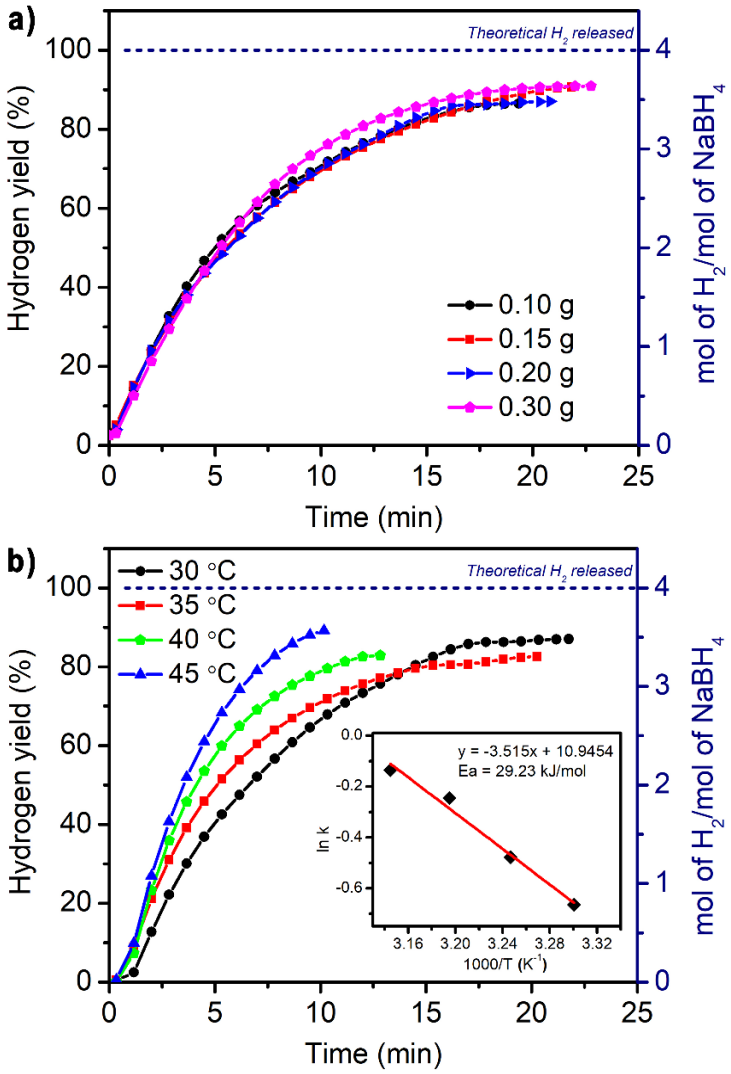

Figure 5. (a) Effect of varying initial $NaBH_4$ dosage on $NaBH_4$ hydrolysis catalysed by 10 wt% Co/BN at 30 °C. (b) Hydrolysis of $NaBH_4$ using 10 wt% Co/BN at four different temperatures with inset showing the corresponding Arrhenius plot.

Table 1. Activation energy (E_a) of Co/BN compared to those of other reported noble and non-noble metal catalysts in the hydrolysis of $NaBH_4$.

Metal	Catalyst	Activation energy, Ea (kJ mol^{-1})	References
Noble metal	Pt–Pd–CNTs	19.0	[38]
	Pt NPs	39.2	[39]
	Ru/TiO_2	62.0	[2]
	Pt/TiO_2	60.5	[2]
	$Ru/Co–TiO_2$	38.7	[7]
Non-noble metal	Co–B/HPCMs	43.3	[9]
	Co–Fe–B	55.6	[12]
	$Ni–B–Cr_{0.8}$	50.6	[13]
	Ni NPs	69.8	[14]
	Co–B/BN	29.2	This work

In general, higher temperatures lead to faster reaction kinetics, which is consistent with chemical kinetics principles. The increased temperature results in a higher kinetic energy and more effective collisions among reactant molecules [36]. Figure 5(b) presents the results of the kinetic study on the hydrolysis of $NaBH_4$ catalyzed by Co–B/BN at various temperatures: 30, 35, 40 and 45 °C. The hydrogen generation curve shows that the reaction rate of $NaBH_4$ hydrolysis was fastest at 45 °C, where all the hydrogen was released in less than 10 min. Using the Arrhenius equation (Equation (9)), the activation energy can be calculated from the slope obtained by the linear fitting of ln k against 1/T.

$$k = Ae^{\frac{-Ea}{RT}} \quad (9)$$

Where k is a rate constant which can be obtained from Equation 8, E_a is the activation energy (kJ mol^{-1}), A is the exponential factor, R is the gas constant (J mol^{-1} K^{-1}) and T is the absolute temperature (K) [37].

Based on the Arrhenius plot (Figure 5(b) inset), the apparent activation energy (E_a) of the reaction catalyzed by Co/BN was determined to be 29.23 kJ mol^{-1}. This suggests that Co–B/BN is a great potential catalyst for hydrogen generation from $NaBH_4$ hydrolysis, demonstrating both high catalytic activity and a lower activation energy compared to other reported studies (Table 1). In this context, Co–B doped with boron nitride (Co/BN) not only exhibited a lower activation energy, indicative of superior catalytic efficiency, but also strikes a balance between cost-effectiveness and stability, making it an ideal candidate for on-demand hydrogen generation in fuel cell applications.

CONCLUSION

In this study, *h*-BN was synthesized using a template-free method and Co–B particles were successfully doped on the surface through chemical reduction with $NaBH_4$, resulting in Co/BN catalysts with evenly distributed active sites. The catalytic performance of BN-supported transition metals followed the order Co/BN > Ni/BN > Cu/BN > Sn/BN, with 10 wt% Co/BN achieving a hydrogen yield of 3.6 mol H_2 mol^{-1} $NaBH_4$ at 30 °C and an activation energy of 29.23 kJ mol^{-1}. The enhanced catalytic performance is attributed to the larger specific surface area of the BN support and the increased number of Co–B particles with more exposed active sites. The rough and porous surface of BN also provides effective anchoring points for Co–B particles, preventing their agglomeration. These findings offer valuable insights into the development of efficient Co-based catalysts for heterogeneous catalytic reactions aimed at hydrogen production using solid phase $NaBH_4$.

ACKNOWLEDGEMENTS

Y.S.C. acknowledges support from Universiti Sains Malaysia, Bridging Grant with Project No: R501-LR-RND003-0000001821-0000.

CONFLICT OF INTEREST

There is no conflict of interest to declare.

REFERENCES

1. Shi, L., Chen, Z., Jian, Z., Guo, F. and Gao, C. (2019) Carbon Nanotubes-Promoted Co–B Catalysts for Rapid Hydrogen Generation via $NaBH_4$ Hydrolysis. *International Journal of Hydrogen Energy*, **44**, 19868–19877.

2. Altaf, C. T., Minkina, V. G., Shabunya, S. I., Colak, T. O., Sankir, N. D., Sankir, M. and Kalinin, V. I. (2023) Ruthenium and Platinum-Modified Titanium Dioxide Support for $NaBH_4$ Hydrolysis. *ACS Omega*, **8**, 36100–36108.

3. Sun, B., Li, X., Zheng, J. (2024) Hydrogen Generation from $NaBH_4$ for Portable Proton Exchange Membrane Fuel Cell. *Materials Reports: Energy*, **4**, 100248.

4. Netskina, O. V., Komova, O. V., Simagina, V. I., Odegova, G. V., Prosvirin, I. P. and Bulavchenko, O. A. (2016) Aqueous-Alkaline $NaBH_4$ Solution: The Influence of Storage Duration of Solutions on Reduction and Activity of Cobalt Catalysts. *Renewable Energy*, **99**, 1073–1081.

5. Simagina, V. I., Ozerova, A. M., Komova, O. V. and Netskina, O. V. (2021) Recent Advances in Applications of Co-B Catalysts in $NaBH_4$-Based Portable Hydrogen Generators. *Catalysts*, **11**, 268.

6. Boran, A., Erkan, S. and Eroglu, I. (2019) Hydrogen Generation from Solid State $NaBH_4$ by using $FeCl_3$ Catalyst for Portable Proton Exchange Membrane Fuel Cell Applications. *International Journal of Hydrogen Energy*, **44**, 18915–18926.

7. Zhang, J., Lin, F., Yang, L. and Dong, H. (2020) Highly Dispersed Ru/Co Catalyst with Enhanced Activity for Catalyzing $NaBH_4$ Hydrolysis in Alkaline Solutions. *Chinese Chemical Letters*, **31**, 2512–2515.

8. Shang, Y. and Chen, R. (2006) Semiempirical Hydrogen Generation Model using Concentrated Sodium Borohydride Solution. *Energy & Fuels*, **20**, 2149–2154.

9. Li, S., Qiu, S., Chua, Y. S., Xia, Y., Zou, Y., Xu, F., Sun, L. and Chu, H. (2024) Co–B Supported on Waxberry-Like Hierarchical Porous Carbon Microspheres: An Efficient Catalyst for Hydrogen Generation via Sodium Borohydride Hydrolysis. *Materials Chemistry and Physics*, **319**, 129399.

10. Ugale, A. D., Ghodke, N. P., Kang, G. S., Nam, K. B., Bhoraskar, S. V., Mathe, V. L. and Yoo, J. B. (2022) Cost-Effective Synthesis of Carbon Loaded Co_3O_4 for Controlled Hydrogen Generation via $NaBH_4$ Hydrolysis. *International Journal of Hydrogen Energy*, **47**, 16–29.

11. Patel, N., Fernandes, R. and Miotello, A. (2009) Hydrogen Generation by Hydrolysis of $NaBH_4$ with Efficient Co–P–B Catalyst: A Kinetic Study. *Journal of Power Sources*, **188**, 411–420.

12. Wang, Y., Zhang, D., Wang, X., Zhang, K., Cao, Z., Qi, N., Wu, S., Bai, S. and Li, G. (2021) Co–Fe–B as an Effective Catalyst for Hydrogen Production from $NaBH_4$ Hydrolysis. *Materials Letters: X*, **12**, 100104.

13. Ababaii, M. A., Gilani, N. and Pasikhani, J. V. (2024) Hydrogen Evolution from $NaBH_4$ Solution using Cr-Doped Ni–B Metallic Catalyst Deposited on Rice Husk via Electroless Plating. *International Journal of Hydrogen Energy*, **51**, 648–662.

14. Ghodke, N. P., Rayaprol, S., Bhoraskar, S. V. and Mathe, V. L. (2020) Catalytic Hydrolysis of Sodium Borohydride Solution for Hydrogen Production using Thermal Plasma Synthesized Nickel Nanoparticles. *International Journal of Hydrogen Energy*, **45**, 16591–16605.

15. Wu, Y., Wu, X., Liu, Q., Huang, C., Qiu, X. (2017) Magnetically Recyclable Ni@h-BN Composites for Efficient Hydrolysis of Ammonia Borane. *International Journal of Hydrogen Energy*, **42**, 16003–16011.

16. Singh, B., Kaur, G., Singh, P., Singh, K., Kumar, B., Vij, A., Kumar, M., Bala, R., Meena, R., Singh, A. and Thakur, A. (2016) Nanostructured Boron Nitride with High Water Dispersibility for Boron Neutron Capture Therapy. *Scientific Reports*, **6**, 35535.

17. Lei, W., Portehault, D., Liu, D., Qin, S. and Chen, Y. (2013) Porous Boron Nitride Nanosheets for Effective Water Cleaning. *Nature Communications*, **4**, 1777.

18. Liu, J. X., Yang, M., Jiang, R. F., Zheng, X. C., Liu, P. (2021) Hexagonal Boron Nitride Supported Ruthenium Nanoparticles as Highly Active Catalysts for Ammonia Borane Hydrolysis. *International Journal of Hydrogen Energy*, **46**, 17708–17719.

19. Liu, K., Yang, S., Chen, Y., Zhang, W., Liu, P., Zheng, X. (2022) Enhanced Catalytic Behavior of h-BN Supported CuNi Bimetallic Catalysts in Hydrolytic Dehydrogenation of NH_3BH_3. *International Journal of Hydrogen Energy*, **47**, 33741–33753.

20. Wu, P., Zhu, W., Chao, Y., Zhang, J., Zhang, P., Zhu, H., Li, C., Chen, Z., Li, H. and Dai, S. (2016) A Template-Free Solvent-Mediated Synthesis of High Surface Area Boron Nitride Nanosheets for Aerobic Oxidative Desulfurization. *Chemical Communications*, **52**, 144–147.

21. Zhang, R., Wang, L., Yang, X., Tao, Z., Ren, X. and Lv, B. (2019) The Role of Surface NH Groups on the Selective Hydrogenation of

Cinnamaldehyde over Co/BN Catalysts. *Applied Surface Science*, **492**, 736–745.

22. Xu, D., Dai, P., Liu, X., Cao, C. and Guo, Q. (2008) Carbon-Supported Cobalt Catalyst for Hydrogen Generation from Alkaline Sodium Borohydride Solution. *Journal of Power Sources*, **182**, 616–620.

23. El Bachiri, A., Soussi, L., Karzazi, O., Louardi, A., Rmili, A., Erguig, H. and El Idrissi, B. (2019) Electrochromic and Photoluminescence Properties of Cobalt Oxide Thin Films Prepared by Spray Pyrolysis. *Spectroscopy Letters*, **52**, 66–73.

24. Chen, Y., Wang, X., Yu, C., Ding, J., Deng, C. and Zhu, H. (2019) Low Temperature Synthesis via Molten-Salt Method of R-BN Nanoflakes, and Their Properties. *Scientific Reports*, **9**, 16338.

25. Sun, X., Yu, T., Chen, Y., Zhang, C., Ma, Z. (2020) Effect of Cobalt on Properties of Vitrified Bond and Vitrified Bubic Boron Nitride Composites. *Ceramics International*, **46**, 5337–5343.

26. Ahmad, P., Khandaker, M. U., Amin, Y. M., Muhammad, N., Usman, A. R., Amin, M. (2015) Effect of Reaction Atmosphere and Growth Duration on Size and Morphology of Boron nitride nanotubes. *New Journal of Chemistry*, **39**, 7912–7915.

27. Min, Y., Zhou, X., Chen, J. J., Chen, W., Zhou, F., Wang, Z., Yang, J., Xiong, C., Wang, Y., Li, F. and Yu, H. Q. (2021) Integrating Single-Cobalt-Site and Electric Field of Boron Nitride in Dechlorination Electrocatalysts by Bioinspired Design. *Nature Communications*, **12**, 303.

28. Guo, J., Hou, Y., Li, B., Liu, Y. (2018) Novel Ni–Co–B Hollow Nanospheres Promote Hydrogen Generation from the Hydrolysis of Sodium Borohydride. *International Journal of Hydrogen Energy*, **43**, 15245–15254.

29. Tan, T., Han, P., Cong, H., Cheng, G. and Luo, W. (2019) An Amorphous Cobalt Borate Nanosheet-Coated Cobalt Boride Hybrid for Highly Efficient Alkaline Water Oxidation Reaction. *ACS Sustainable Chemistry & Engineering*, **7**, 5620–5625.

30. Zhu, Y., Yu, L. Z., Wang, F., Xu, J., Xue, B. (2023) Solvent-free Selective Oxidation of Ethylbenzene with Molecular Oxygen Catalyzed by Cobalt Catalysts Supported on Exfoliated Carbon Nitride. *ChemistrySelect*, **8**, e202301526.

31. Wang, J. (2025) Study on the Catalytic Mechanism of Core-Shell Structure CoCu@BN Promoting the Hydrolytic Dehydrogenation of Ammonia Borane. *International Journal of Hydrogen Energy*, **158**, 150409.

32. Hua, D., Hanxi, Y., Xinping, A. and Chuansin, C. (2003) Hydrogen Production from Catalytic Hydrolysis of Sodium Borohydride Solution using Nickel Boride Catalyst. *International Journal of Hydrogen Energy*, **28**, 1095–1100.

33. Wang, W., Zhao, Y., Chen, D., Wang, X., Peng, X. and Tian, J. (2014) Promoted Mo Incorporated Co–Ru–B Catalyst for Fast Hydrolysis of $NaBH_4$ in Alkaline Solutions. *International Journal of Hydrogen Energy*, **39**, 16202–16211.

34. Kaur, A., Gangacharyulu, D. and Bajpai, P. K. (2019) Kinetic Studies of Hydrolysis Reaction of $NaBH_4$ with γ-Al_2O_3 Nanoparticles as Catalyst Promoter and $CoCl_2$ as Catalyst. *Brazilian Journal of Chemical Engineering*, **36**, 929–939.

35. Demirci, U. B. and Miele, P. (2014) Reaction Mechanisms of the Hydrolysis of Sodium Borohydride: A Discussion Focusing on Cobalt-Based Catalysts. *Comptes Rendus Chimie*, **17**, 707–716.

36. Mirshafiee, F. and Rezaei, M. (2023) Co/Fe_3O_4 @GO Catalyst for One-Step Hydrogen Generation from Hydrolysis of $NaBH_4$: Optimization and Kinetic Study. *International Journal of Hydrogen Energy*, **48**, 32356–32370.

37. Goh, J. D., Lee, H. L. and Chua, Y. S. (2019) Palladium (II) Chloride Catalytic Methanolysis of Hydrazine Borane for Enhanced Hydrogen Production. *Journal of Physical Science*, **30**, 127–139.

38. Pena-Alonso, R., Sicurelli, A., Callone, E., Carturan, G. and Raj, R. (2007) A Picoscale Catalyst for Hydrogen Generation from $NaBH_4$ for Fuel Cells. *Journal of Power Sources*, **165**, 315–323.

39. Huff, C., Biehler, E., Quach, Q., Long, J. M., Abdel-Fattah, T. M. (2021) Synthesis of Highly Dispersive Platinum Nanoparticles and Their Application in a Hydrogen Generation Reaction. *Colloids and Surfaces A: Physicochemical and Engineering Aspects*, **610**, 125734.